SAND2016-7592C

Hierarchical Multi-Scale Approach to Validation and Uncertainty Quantification of Hyper-Spectral Image Modeling

David W. Engel[1a], Thomas A. Reichardt[b],
Thomas J. Kulp[b], David L. Graff[c], and Sandra E. Thompson[a]
[a]Pacific Northwest National Laboratory: 902 Battelle Blvd, Richland, WA, 99354
[b]Sandia National Laboratories: P. O. Box 969, Livermore, CA, 94551
[c]Los Alamos National Laboratory: P. O. Box 1663, Los Alamos, NM, 87545

ABSTRACT

Validating predictive models and quantifying uncertainties inherent in the modeling process is a critical component of the *HARD Solids Venture* program [1]. Our current research focuses on validating physics-based models predicting the optical properties of solid materials for arbitrary surface morphologies and characterizing the uncertainties in these models. We employ a systematic and hierarchical approach by designing physical experiments and comparing the experimental results with the outputs of computational predictive models. We illustrate this approach through an example comparing a micro-scale forward model to an idealized solid-material system and then propagating the results through a system model to the sensor level. Our efforts should enhance detection reliability of the hyper-spectral imaging technique and the confidence in model utilization and model outputs by users and stakeholders.

Keywords: Validation, uncertainty quantification, calibration, sensitivity analysis, hyper-spectral imaging

1. INTRODUCTION

Identifying and applying appropriate validation and uncertainty quantification (V/UQ) methods is instrumental in strengthening the validity and scientific rigor of predictive modeling of the hyperspectral imaging (HSI) observables associated with solid particulate materials. Validating these predictive models and quantifying uncertainties inherent in the modeling process presents a significant research challenge.

In this paper, we present techniques for validating physics-based models that predict HSI observables of solid particulate materials and characterizing model uncertainties. We are employing a hierarchical V/UQ approach by designing physical experiments and comparing the experimental results with the outputs of computational predictive models. We illustrate this approach by comparing a model for the reflectance of a particulate material to the reflectance spectrum acquired on a well-characterized particulate deposit. We then take the results at this lower scale (micro-scale) and propagate it through a system-level model to start to understand how uncertainties at the lower scales affect results at the upper scale (sensor). By validating physical models with experimental data at various scales, and characterizing and quantifying uncertainties in the modeling process, we anticipate that incorporation of V/UQ techniques will elevate the level of confidence stakeholders have in model utilization and model outputs.

2. VALIDATION/UQ PROCESS

The validation process that we are incorporating is shown in Figure 1. The key elements of this process are verification, uncertainty quantification (UQ), validation (or comparison), and model maturity. Verification addresses the correctness and functionality of the computations and denotes the process of establishing the precision of the numerical solution of the computational model in comparison to the "true" analytical solution [2]. Model verification is important for ensuring that the computer program of the computerized model and its implementation are correct. Validation is a critical process for determining the degree to which a model is an accurate representation of the real processes [3]. The purpose of model validation is to substantiate that a computerized model possesses a satisfactory range of accuracy consistent with the intended application of the model. Uncertainty Quantification is the process of quantifying uncertainties that arise in the computational modeling, or prediction process, in this case, of physical systems [4]. Sources of uncertainty may include

[1] dave.engel@pnnl.gov, (509) 375-2307

input model parameters, internal model parameters, numerical errors (estimated during verification), and model bias (estimated during validation). The process known as predictive maturity [5] tries to answer the following questions

- Are further experiments needed?
- Has the maturity of the model reached a level where no more significant reduction in uncertainty is attained or worthwhile?
- Has the figure of merit (efficiency and effectiveness) been reached?

For this paper, the primary focus is on UQ, including calibration, sensitivity analysis (SA), and uncertainty analysis (UA), shown in the light blue shaded boxes on the left side in Figure 1. As Figure 1 illustrates, the differences resulting from comparing modeled results and experimental observations determine the path(s) to model refinements, i.e. by improving the physics models, by collecting and incorporating more data into the existing model, or both. Such iterative comparisons provide continuous feedback into the modeling and UQ process until the differences between the modeled results and experimental observations become sufficiently small.

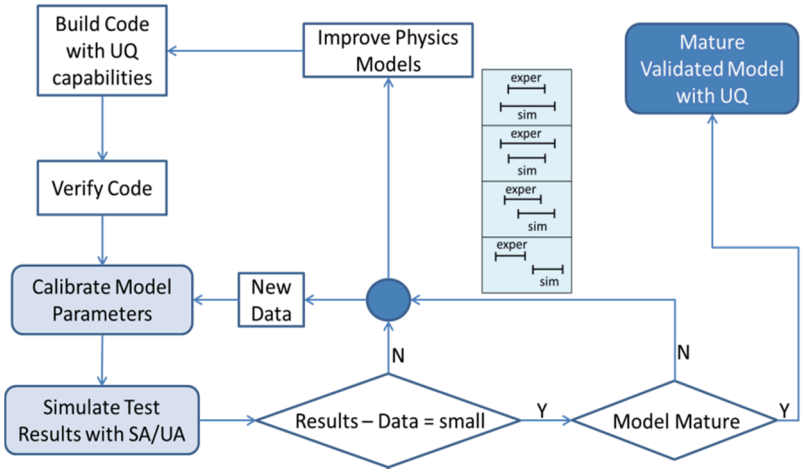

Figure 1. Model validation process, which includes verification, UQ, and model maturity.

For complex multi-physics problems like modeling the HSI observables of particulate materials, a hierarchical approach is needed due to limited feasibility of designing and conducting accurate validation and UQ experiments on full-scale systems. To generate comparisons between modeling and experimental results, we apply such a hierarchical approach to designing physical experiments (and/or utilizing available measurement data sets) to compare with the results of predictive computational models. This approach divides a system analysis into several progressively smaller scales—the system scale (i.e., the full HSI data cube that is acquired by the sensor), the individual-pixel scale of the data cube, the micro-scale (i.e. at the level of interaction of electromagnetic radiation with the particulate medium), and the intrinsic material properties (i.e., the complex refractive index $n+ik$ of the material, its measurement often requiring the application of models as well) —to identify and quantify measured simulation errors against experimental data and to provide a quantitative assessment of uncertainties. This hierarchy is illustrated in Figure 2 by the data flow through the different models at different scales. We enable scalability by utilizing both forward and inverse modeling. The left side of Figure 2 illustrates the forward (up scale) data and model flow from intrinsic optical properties all the way up to the sensor level (data cube). The right hand side of Figure 2 then starts with the sensor data and propagates the results for materials of interest (MOI) down scale back to the intrinsic properties of the material. This hierarchical approach leverages smaller scale models and data to investigate the accuracy of the various components of the system so that lower-level analysis can inform V/UQ on a larger scale.

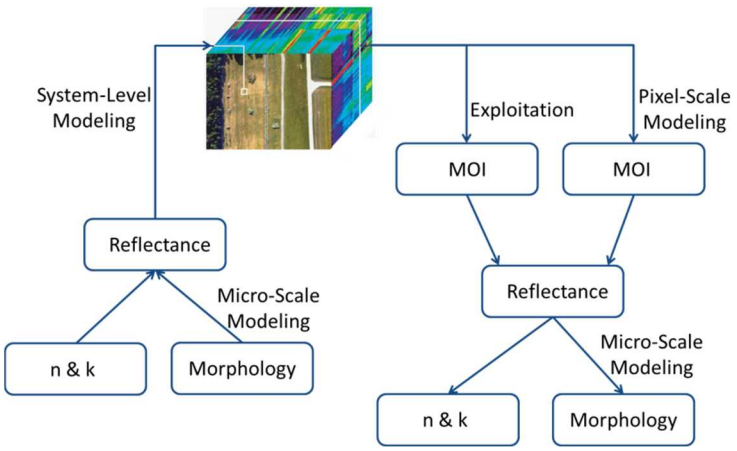

Figure 2. Data and model flow for the HSI material identification problem.

The outcome of this V/UQ process will be estimates of input parameter uncertainties for each calibrated model, the confidence range of model output at each scale, and the uncertainty of the overall system response (i.e., sensor data). These estimates will be based on the confidence levels developed in the various decoupled scale problems as well as the upscaling procedure. By considering smaller scale problems that isolate particular aspects of the multi-physics of the full scale system, we should be able to evaluate and isolate the contributions of different aspects of the model to the predictive errors, such as the effects of coupling different physics or the geometric upscaling of the coupled physics. In the following section, we use a micro-scale model to demonstrate the utility of using a lower-level model to inform UQ at a higher level.

3. MICRO-SCALE MODEL

To illustrate the V/UQ process, we focus the majority of our analysis on a single physical scale—the micro-scale. It is well known that the reflectance spectrum of a particulate medium can depend strongly upon the size of the particulates [6][7], and that the nature of this dependence is a function of the material refractive index. To account for this dependence, we implement a reflectance model developed for an optically thick particulate deposit with corrections for particle packing density and particle shape effects [8]. The model approximates the range of particle size in the deposit with a bimodal volume log-normal [9] particle size distribution (PSD). The analyses performed with the micro-scale model were done using the Dakota software tools [10].

3.1 Model Optimization

An optimization analysis was performed on the micro-scale model to estimate the input parameters that best fit laboratory measured fused silica reflectance [11], with the goal of calibrating model parameters to best approximate material morphology when the material type and the reflectance are known. The micro-scale model utilizes eight input parameters, including:

1) r_g, the characteristic particle radius of the large-particle mode of the PSD
2) $[\ln(\sigma_g)]^2$, the width of the large-particle mode of the PSD
3) r_g, the characteristic particle radius of the small-particle mode of the PSD
4) $[\ln(\sigma_g)]^2$, the width of the small-particle mode of the PSD
5) γ, the population ratio between the two modes
6) particle fill factor to account for the impact of packing density on particle scattering within the medium
7) angle bin # for the angle of incidence, varied to account for surface roughness effects
8) Fresnel-like component resulting from impact of packing density on the first-surface reflection

For an initial assessment of model validity, we focus on the first five parameters associated with the PSD, comparing the PSD calculated from optimized parameters to PSDs measured via laser diffraction. We display one such set of comparisons in Figure 3. Optimization of the reflectance model to the measurement of a reflectance spectrum of a silica particulate deposit (Figure 3, left) yields a PSD consistent with independent laser-diffraction measurements of the particle population (Figure 3, right), demonstrating that the numerically invertible model can extract approximate morphology when material type and reflectance are known.

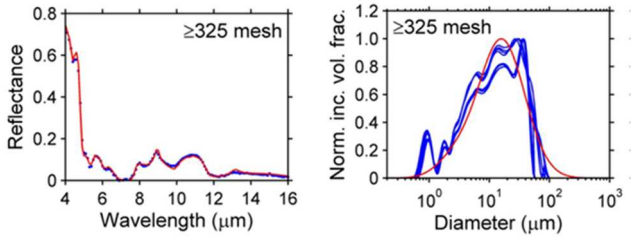

Figure 3. Results of optimization: left is reflectance, right is particle size distribution, blue curves are measured results and the red curves represent model results.

4. UNCERTAINTY QUANTIFICATION

The optimization (calibration) exercise discussed above showed that a good agreement (visually) is obtainable using the micro-scale model results and laboratory data. However, in real world applications, larger uncertainties stemming from multiple sources can be difficult to capture and thus require more complex approaches to modeling uncertainties. Below we describe a stochastic approach to uncertainty modeling.

4.1 Bayesian Calibration

To estimate uncertainties with the model input parameters, a Bayesian-like calibration can be used to explicitly deal with (1) treatment of functional output, (2) emulation of the model (functional) output, and (3) calibration parameter screening and selection [12]. In Bayesian calibration, uncertain input parameters are described by a "prior" distribution. The priors are updated with experimental data in a Bayesian framework that involves the experimental data and a likelihood function which describes how well each parameter value is supported by the data. The posterior distribution is the distribution for the input parameters after taking into account the observed data. This posterior distribution can be determined by Bayes' rule [12], as shown in Eq. 1.

$$p(\theta|\, X,\, \alpha) \propto\ p(X\,|\theta)\, p(\theta,\, \alpha) \tag{1}$$

Where the sampling distribution, $p(X|\theta)$, is the distribution of the observed data conditional on its parameters (also called the likelihood function), $p(\theta,\alpha)$ is the prior parameter distributions, and α is a hyper parameter (parameter of the prior distribution). This posterior distribution is then proportional to its likelihood multiplied by its prior distribution. The likelihood function is derived from a statistical model for the observed data. Once we have the prior and the likelihood, the posterior distribution is calculated from an integral. This integral is typically approximated using a numerical technique, such as Markov Chain Monte Carlo (MCMC) [13].

The results of a Bayesian calibration analysis for the same example from the optimization exercise are shown in Figure 4. The prior distributions are represented by the blue dash lines, the posterior distributions are represented by the histograms, with a beta distribution being fit to each histogram (red curves). For this analysis, 150 functional evaluations were performed using the prior distributions shown in Figure 4 and a Latin Hypercube sampling design [14]. A Gaussian Process (GP) model was then fit to the functional evaluations to be used as a surrogate model (emulator) [15]. An MCMC analysis with 5000 iterations was then performed using the GP model to best fit the measured data.

4.2 Sensitivity Analysis

After calibration, a sensitivity analysis (SA) was performed to further understand the model, i.e., to ascertain which model parameters contribute the most to the uncertainty in the output, and to ensure that the model behaves as expected when model parameters vary [16]. A simple SA was performed using the posterior distributions from the calibration and

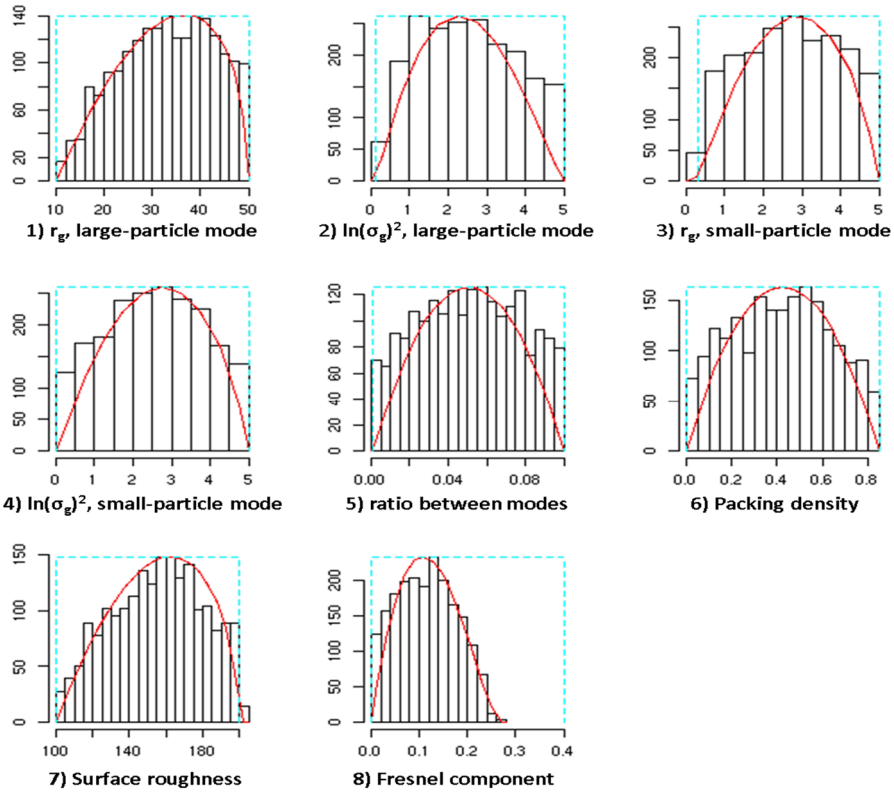

Figure 4. Calibration results: blue dash lines are prior distributions for each parameter, histograms are posterior distributions and red curves are beta distributions fit to the histograms.

the Morris design [17]. In this design, only one parameter value is changed and the model is run (one-at-a-time). A compilation of this analysis is shown in Figure 5.

The SA utilized a very simple design, which nonetheless revealed added insights. For instance, changing values for parameters 3-5 had very little effect on reflectance, indicating that the primary impact of particle size is associated with the large particle mode of the PSD. While changes in parameters 1, 2, 6, and 7 had noticeable effects on the change in reflectance, the change in parameter 8 had a much larger effect that appears to impact the spectral features (between 8 and 10 μm) that could likely impact minimal detectable quantity that a detection algorithm would target. This is consistent with the reported strong impact of particle packing density on changes in the reflectance due to the Fresnel-like component [18]. The analysis also pointed to anomalous model results when the packing density (parameter 6) was large for wavelengths between 5-6 μm (green curve), likely associated with a limited range of numerical applicability in the computation used to account for the impact of packing density on particle scattering within the medium.

A separate sensitivity analysis using the MCMC results is shown in Figure 6. For this analysis, the resulting variable is the sum of squared errors (SSE) between the simulated reflectance and the measured reflectance. The resulting variable is analyzed against each input parameter and plotted in Figure 6. In each scatter-plot a regression analysis is shown (red line) to estimate the correlation. These results show that parameters 1 and 3-6 show very little correlation with the resulting SSE, parameters 2 and 7 show a slight correlation, and parameter 8 shows the most correlation of all the parameters. These results are similar to the SA using the Morris design.

Also shown in each scatter-plot of Figure 6 are the five best MCMC results. These (MCMC) runs are marked by the colored circles and represent the simulated spectra with the smallest SSE. The results of the optimization analysis (Figure 3) are marked by an **X** in each scatter-plot. These results illustrate the many local minima of the functional results, and help to explain why the ranges of the posterior parameter distributions resulting from the Bayesian calibration were not much different from the prior distributions.

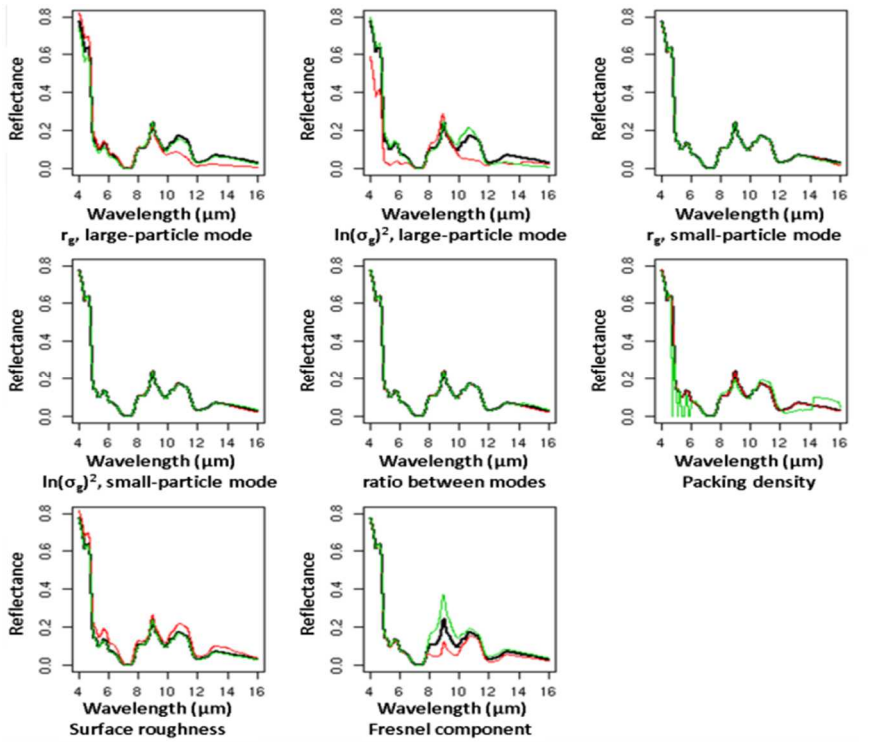

Figure 5. Sensitivity analysis using a one-at-a-time design. Green curves represent modeled reflectance when the larger parameter value is used; red curves represent using the smaller parameter; black curves represent using parameter means.

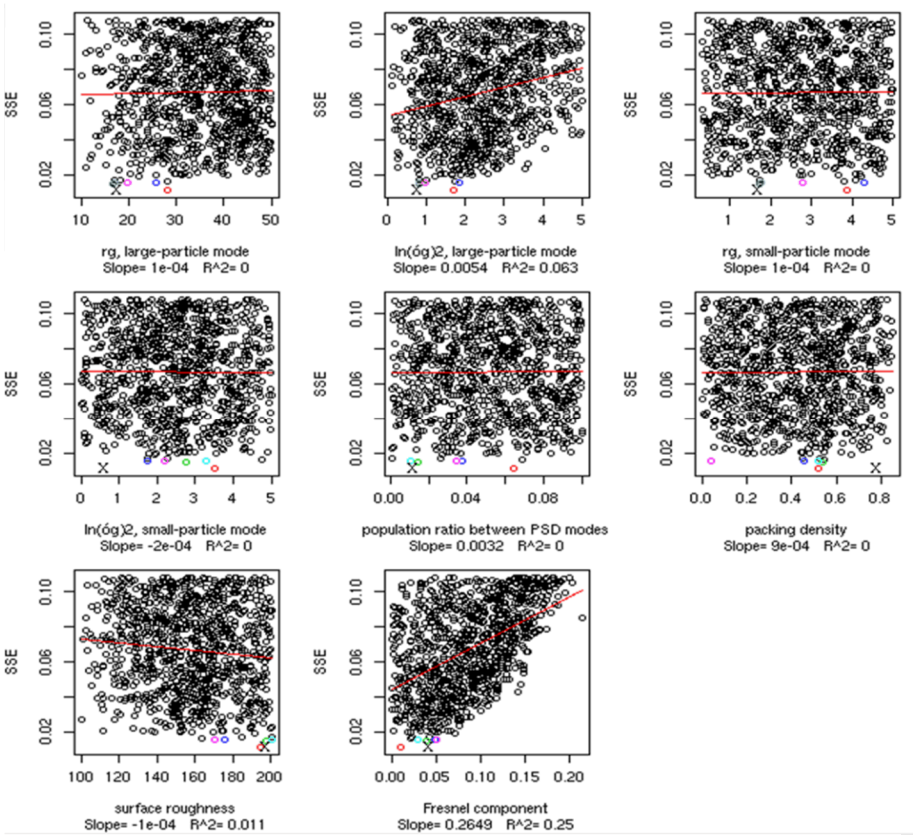

Figure 6. Sensitivity analysis using the MCMC analysis results.

4.3 Uncertainty Analysis

Uncertainty analysis (UA) refers to the process of propagating the uncertainty in the model parameters through to the outputs of interest to obtain a distribution of model output. Utilizing the posterior parameter distributions extracted from the calibration exercise, a Monte Carlo simulation was performed to estimate the output uncertainties. The top 1000 results are shown in Figure 7. These spectra represent the closest 1000 model results to the measured spectra used in the calibration exercise. Importantly, these uncertainties assume both the PSD and the Fresnel-like component are unknown, so the results emphasize the impact of these parameters on the HSI observable.

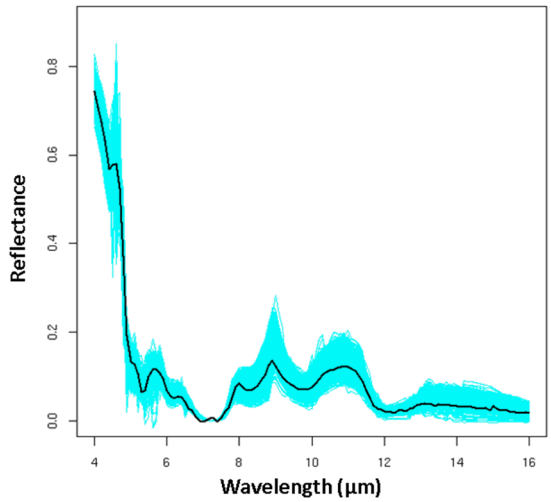

Figure 7. Uncertainty analysis based on the calibration posterior parameter distributions. Blue curves represent the top 1000 modeled spectra, while the black curve represents the measured results.

5. Sensor-Scale Modeling

Ultimately we are interested in evaluating the optical properties of particulate materials as a potential observable for HSI systems. It is straightforward to extend the above analysis to predict the sensitivity of an airborne LWIR HSI sensor through the use of a physics-based, end-to-end, system-level modeling and simulation tool for optical hyperspectral remote sensing instruments. For this analysis, we selected 25 spectra from the previous 5000 UQ runs and predicted the sensor output with a modeled atmosphere. These 25 spectra were randomly selected from the results shown in Figure 7 using a stratified sampling design. We chose a set of system parameters that are typical of an airborne collection: a generic LWIR HSI pushbroom sensor observing a pure pixel of material with a fixed ground temperature of 300 K, from a fixed altitude of 4 km, and through a US 1976 Standard atmosphere, as calculated by MODTRAN [19]. The results of the system-scale modeling are shown in Figure 8 and illustrate the sensitivity of an airborne sensor to changes in the optical properties of the observed materials. In particular, the sensitivity to these effects is most pronounced closer to the center of the LWIR window, where the transmission of the atmosphere is less cluttered by strong atmospheric absorbers.

6. CONCLUSION

In this paper, we introduce a hierarchical approach to validating a multi-scale model for predicting HSI observables from solid particulate materials, and illustrate techniques for quantifying uncertainties in the complex modeling process. We describe an iterative process of using comparative differences between experimental observations and model results to evaluate model validity. Using a single-scale model as a proof-of-concept example, we demonstrate the feasibility of the Bayesian approach to modeling uncertainty at the micro scale. These lower scale UQ results were then propagated up to the sensor level to illustrate possible effects of modeled uncertainties to HSI images. We also show that sensitivity and uncertainty analysis, as part of our approach, generated added insight into anomalies in the modeling, which can provide valuable feedback to model developers and experimentalists. Our work helps address UQ within the HSI model application domain and, with continuing efforts, will help researchers and stakeholders gain greater confidence in the utility and defensibility of multi-scale physical models and model outputs.

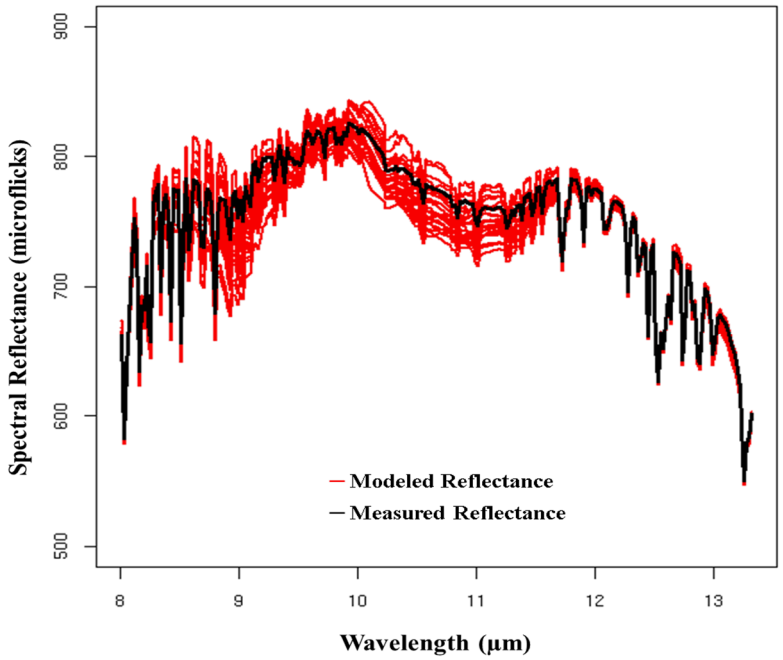

Figure 8. Propagation of UQ results (red curves) and measured results (black curve) at the micro scale to the sensor level.

ACKNOWLEDGEMENT

This research was supported by the U.S. Department of Energy (DOE) National Nuclear Security Administration (NNSA) Office on Nonproliferation and Verification Research and Development (DNN R&D). The Pacific Northwest National Laboratory is operated by Battelle for the U.S. DOE under contract DE-AC05-76RL01830. Sandia is a multi-program laboratory operated by Sandia Corporation, a wholly owned subsidiary of Lockheed Martin Company, for the U.S. DOE National Nuclear Security Administration under contract DE-AC04-94AL85000. Los Alamos National Laboratory, an affirmative action/equal opportunity employer, is operated by the Los Alamos National Security, LLC, for the National Nuclear Security Administration of the U.S. DOE under contract DE-AC52-06NA25396.

REFERENCES

[1] Peltz, J. J., Strasburg, J. D. and Thompson, S. E., "Hard solids: Addressing spectral challenges through modeling," Proc. SPIE, 9840-15 (2016).

[2] Oberkampf, W. L. and Roy, C. L., [Verification and validation in scientific computing], Cambridge University Press, Cambridge, UK (2010).

[3] Oberkampf, W. L. and Barone, M. F., "Measures of agreement between computation and experiments: validation metrics," Computational Physics – Special issue: Uncertainty quantification simulation sciences, 217, 5-36 (2010).

[4] Ghanem, R. G., "Uncertainty Quantification in Computational and Prediction Science," Numerical Methods in Engineering, 80, 671-672 (2009).

[5] Hemez, F., Sezer Atamturktur, H. and Unal, C., "Defining predictive maturity for validated numerical simulations," Computers and Structures, 88, 497–505 (2010).

[6] Myers, T. L., Brauer, C. S., Su, Y.- F., Blake, T. A., Tonkyn, R. G., Ertel, A. B., Johnson, T. J. and Richardson, R. L., "Quantitative reflectance spectra of solid powders as a function of particle size," Appl Opt, 54, 4863-4875 (2015).

[7] Moersch, J. E. and Christensen, P. R., "Thermal emission from particulate surfaces: A comparison of scattering models with measured spectra," J. Geophys. Res., 100(E4), 7465-7477 (1995).

[8] Reichardt, T. A. and Kulp, T. J., "Radiative transfer modeling of surface chemical deposits," Proc. SPIE, 9840-21 (2016).

[9] Mishchenko, M. I., Travis, L. D. and A. A., Lacis, [Scattering, absorption, and emission of light by small particles], Cambridge University Press, Cambridge, U.K. (2002).

[10] Adams, B. M., Bauman, L. E., Bohnhoff, W. J., Dalbey, K. R., Eddy, J. P., Ebeida, M. S., Eldred, M. S., Hough, P. D., Hu, K. T., Jakeman, J. D., Swiler, L. P., Stephens, J. A., Vigil, D. M. and Wildey, T. M., "Dakota, a multilevel parallel object- oriented framework for design optimization, parameter estimation, uncertainty quantification, and sensitivity analysis: Version 6.1 reference manual," Technical Report SAND2014-5015, Sandia National Laboratories, Albuquerque, NM (2014).

[11] Kulp, T. J., Sommers, R. L., Murtagh, D., Krafcik, K. L., Mills, B. E., Reichardt, T. A., LaCasse, C. F., Fuerschbach, K. H. and Craven-Jones, J., "Ideal system morphology and reflectivity measurements for model development and validation," Proc. SPIE, 9840-16 (2016).

[12] Kennedy, M. and O'Hagan, A., "Bayesian calibration of computer models (with discussion)," Royal Statistical Society, B63, 425-464 (2001).

[13] Hastings, W. K., "Monte Carlo sampling methods using Markov chains and their applications," Biometrika, 57(1), 97–109 (1970).

[14] Helton, J. and Davis, F., "Latin Hypercube sampling and the propagation of uncertainty in analysis of complex systems," Reliability Engineering and System Safety, 81, 23-69 (2003).

[15] Santner, T. J., Williams, B. J. and Notz, W. I., [The Design and Analysis of Computer Experiments], Springer, New York (2003)

[16] Saltelli, A., Tarantola, S., Campolongo, F. and Ratto, M., [Sensitivity analysis in practice a guide to assessing scientific models], John Willy & sons, Ltd: 94–120 (2004).

[17] Morris, M. D., "Factorial sampling plans for preliminary computational experiments," Technometrics, 33: 161–174. doi:10.2307/1269043 (1991).

[18] Salisbury, W. and Wald, A., "The role of volume scattering in reducing spectral contrast of Reststrahlen bands in spectra of powdered minerals," Icarus 96, 121-128 (1992).

[19] Berk, A., Anderson, G. P., Acharya, P. K., Bernstein, L. S., Muratov, L., Lee, J., Fox, M. J., Adler-Golden, S. M., Chetwynd, J. H., Hoke, M. L., Lockwood, R. B., Cooley, T. W. and Gardner, J. A., "MODTRAN5: a Reformulated Atmospheric Band Model with Auxiliary Species and Practical Multiple Scattering Options," SPIE Int. Soc. Opt. Eng., 5655, 88 (2005).